



17th International Conference on Metal Forming, Metal Forming 2018, 16-19 September 2018,  
Toyohashi, Japan

## Visualization of strain distribution in tensile test of ferrite + martensite multilayered steel sheet by digital image correlation method

Norimitsu Koga<sup>a,\*</sup>, Masayuki Suzuki<sup>b</sup>, Osamu Umezawa<sup>a</sup>

<sup>a</sup>Faculty of engineering, Yokohama National University, 79-5 Tokiwadai, Hodogaya, Yokohama, Kanagawa, 240–8501, Japan.

<sup>b</sup>Graduate school of engineering, Yokohama National University, 79-5 Tokiwadai, Hodogaya, Yokohama, Kanagawa, 240–8501, Japan.

---

### Abstract

A strain distribution introduced by tensile deformation in a ferrite + martensite multilayered steel was visualized using the digital image correlation method and its local deformation and fracture behavior were characterized. The strain was continuously distributed along 45 degrees from the tensile direction regardless of the layers and was predominately to concentrate in martensite layers. Voids or cracks were generated from highly strained martensite layers and their coalescence led to the fracture. Therefore, the deformability and ductility of hard layer play an important role in the deformation and fracture in a multilayered steel.

© 2018 The Authors. Published by Elsevier B.V.

Peer-review under responsibility of the scientific committee of the 17th International Conference on Metal Forming.

*Keywords:* Multilayered steel; Strain distribution; Digital image correlation; Tensile deformation; Fracture behavior

---

### 1. Introduction

A multilayered material consists of hard and soft layers aligned in parallel along rolling direction and it is designed for improving the toughness of a hard layer to combine them with a soft layer. Koseki et al. [1] demonstrated that a multilayered steel has superior tensile properties to a multiphase steel's one such as a dual phase steel and transformation induced plasticity steel. In addition, they revealed that tensile properties of each layer influence on the

---

\* Corresponding author. Tel.: +81-45-339-3873; fax: +82-45-339-3873

E-mail address: [koga-norimitsu-sx@ynu.ac.jp](mailto:koga-norimitsu-sx@ynu.ac.jp)

strength and ductility of a multilayered steel. This influential factor on tensile properties is similar to that of dual phase steel [2]. On the other hands, Ojima et al. [3] investigated strain partitioning behavior during tensile deformation between hard and soft layers in a multilayered steel by using in-situ-neutron diffraction method. They revealed that there are three deformation stages: a fully elastic stage where both phases deform elastically, a partially plastic stage where soft layers yield while hard layers continue to deform elastically, and a fully plastic stage where yielding occurs in both phases. These deformation stages had also been observed in dual phase steel [4] though applied strain is more efficiently transferred to hard layer in a multilayered steel compared to a dual phase steel. These results imply that a multilayered steel exhibits similar deformation behavior to a dual phase steel's one macroscopically and a good strength-ductility balance in a multilayered steel may relate to its local deformation and fracture behavior.

The digital image correlation method which calculates strain from the difference of images before and after deformation has been developed as a conventional strain analysis [5, 6]. This method has an advantage to apply to any materials and strain modes as long as a significant contrast in a digital image and calculates not only accurate strain but also these distributions. Macroscopic strain distribution introduced by various deformation modes has been visualized [7]. Recently, the digital image correlation using high magnification scanning electron microscopy digital images successfully demonstrated that it was effective to reveal the relation between strain distribution and microstructure. Nakada et al. [8] revealed that strain is hierarchically distributed in each scale and strain concentration in ferrite phase at ferrite/martensite interfacial boundary occurs in a tensile deformed ferrite + martensite dual phase steel by applying digital image correlation method to various magnification scanning electron microscopy images. These strain concentration should lead to nucleation of voids or cracks in a dual phase steel because it has been observed that voids or cracks form at ferrite/martensite interfacial boundary [9]. On the other hands, in a multilayered steel sheet, since ferrite/martensite interfacial boundary is aligned in parallel along rolling direction, strain concentration and void or crack nucleation behavior should be different from that of a dual phase steel in which hard phase is randomly distributed.

In this study, strain distribution developed after tensile deformation in a ferrite + martensite multilayered steel sheet was visualized by digital image correlation method and its local deformation and fracture behavior was characterized.

## 2. Experimental procedure

A commercial ferrite + martensite multilayered steel sheet was used in this study. The specimen was solution treated at 1273 K for 3.6 ks and subsequently water quenched. Microstructure was observed on a longitudinal section using field emission scanning electron microscopy and crystal orientation was analyzed by means of electron backscattered diffraction. Electron backscattered diffraction data were analyzed with the software program OIM™ analysis 7.0.1 for phase and crystal orientation determination. Micro Vickers hardness test was individually performed on ferrite and martensite layers under 0.01 N and 0.005 N load, respectively. The test specimens for tensile test and digital image correlation analysis were machined according to the dimensions in Fig. 1(a) and (b). Tensile testing was done at an initial strain rate of approximately  $2.8 \times 10^{-4} \text{ sec}^{-1}$  at 293 K and the tensile axis corresponds to rolling direction of the specimen. The digital image correlation analysis was carried out using VIC-2D software (Correlated Solutions Inc.) for scanning electron microscopy images before and after 1.6 % and 7.2 % tension specimens under 61 pixels in subset and 5 pixels in step. Scanning electron microscopy images for digital image correlation analysis were obtained from transverse direction section of the specimen shown in Fig. 1(b).

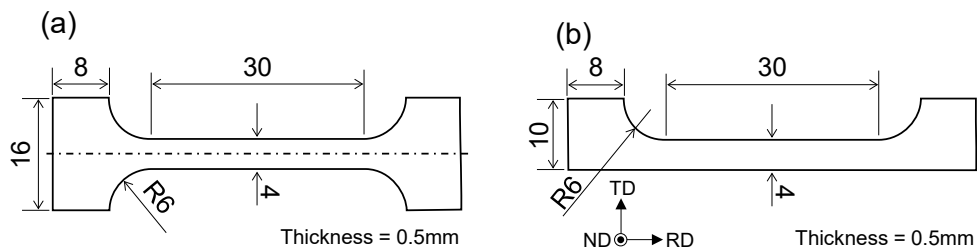


Fig. 1. Configurations of (a) tensile test specimen and (b) digital image correlation analysis one.

### 3. Results and discussion

#### 3.1. Microstructure and tensile property

Fig. 2 shows scanning electron microscopy image (a), inverse pole figure in bcc phase (b) and kernel average misorientation map (c) on transverse direction section after heat-treatment. Each color in (b) and (c) corresponds to crystal orientation on rolling direction and kernel average misorientation value, respectively. Martensite layers were aligned in parallel along rolling direction, and there were no peel off or voids at ferrite/martensite interface boundary. Volume fractions, number of layers, width of layers estimated from the scanning electron microscopy image (a) and Vickers hardness measured on each phase were summarized on Table. 2. Ferrite layer had larger volume fraction and width than martensite layers' one and hardness of ferrite layers was less than half of hardness of martensite layers. Martensite layer has small acicular grains that are similar to a lath martensite structure observed by electron backscattered diffraction method [10]. Kernel average misorientation value within martensite layers was higher than that within ferrite layer as shown in (c), which means martensite layer has a certain strain because it had been demonstrated that kernel average misorientation map tends to correspond to strain distribution map [11]. Fig. 3 is standard stereo-triangle plotting intensity of crystal orientation on rolling direction in the ferrite (a) and martensite (b) layer. There are no high intensity crystal orientation in martensite layer, therefore, crystal orientation is randomly distributed. While ferrite layer exhibits strong  $\{101\}$  texture which may be developed during cold rolling and retain even after recrystallization. Fig. 4 is nominal stress - strain curve and true stress and work hardening rate as a function of true strain. The multilayered steel shows continuous yielding and high work-hardening rate at an early stage of deformation.

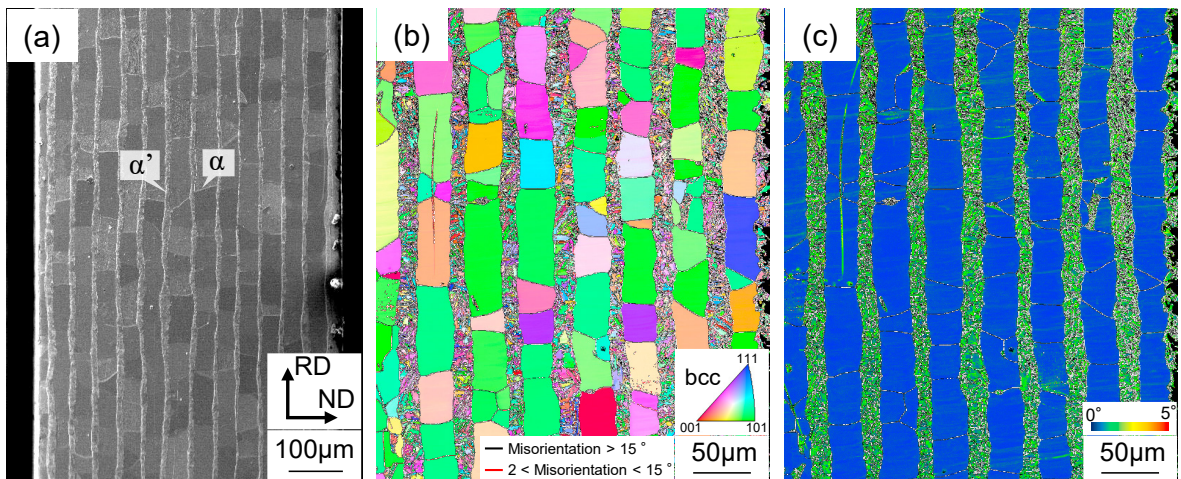


Fig. 2. (a) Scanning electron microscopy image; (b) inverse pole figure in bcc phase; (c) kernel average misorientation map on transverse direction section after heat-treatment in ferrite + martensite multilayered steel.

Table.1. Characteristics of ferrite and martensite multilayered steel.

	Volume fraction [%]	Number of layres [-]	Width of layer [μm]	Vickers hardness [HV]
Ferrite phase	72.4	14	32.9	194
Martensite phase	27.6	13	9.7	554

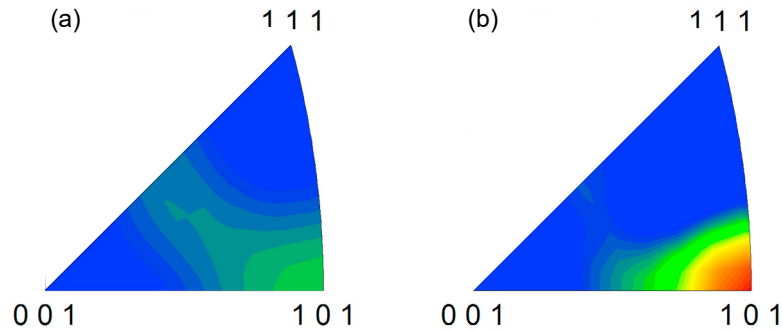


Fig. 3. Standard stereo-triangle plotted intensity of each crystal orientation on rolling direction direction in (a) ferrite and (b) martensite layers.

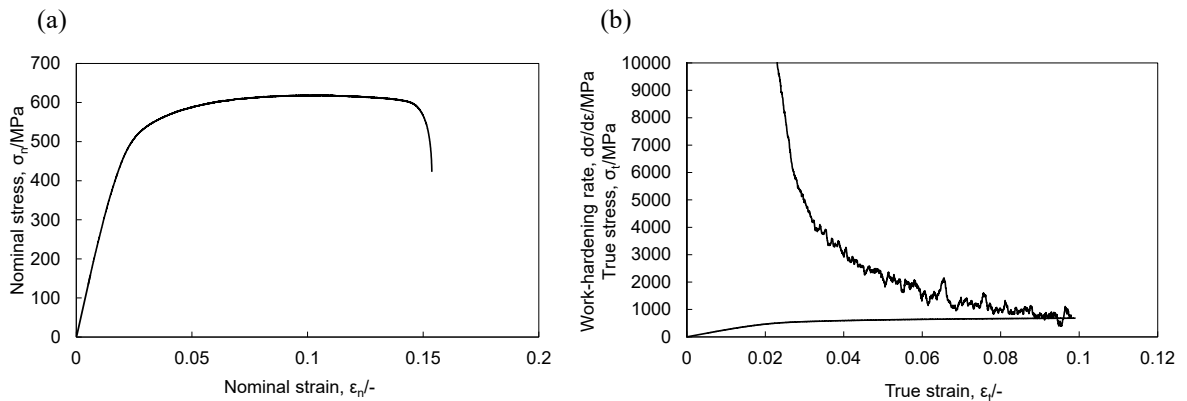


Fig. 4. (a) Nominal stress – strain curve and (b) true stress and work hardening rate and true strain.

### 3.2. Deformation and fracture behavior

Fig. 5 shows  $\epsilon_{xx}$  strain distribution in low and high magnification scanning electron microscopy images after 1.6 % (a), (b) and 7.2 % (c), (d) tensile strain in the multilayered steel. Each color in the maps corresponds to strain, minimum and maximum strain in color bar are 0 and approximately twice as much as average strain, respectively. White dash lines indicate ferrite/martensite layer boundary, and subset size is represented by a black square in each map. Strain was inhomogeneously distributed: high strain region was over twice as much as average strain and low strain region was 0. These high and low strain regions tend to be continuously distributed along 45 degrees from the tensile direction regardless of the layers. Similar deformation behavior had been observed in polycrystalline ferrite single phase steel [12], therefore, it can be concluded that ferrite and martensite layers are simultaneously deformed in the multilayered steel despite of significant difference of hardness between these layers. High strain regions were located at not ferrite/martensite layer boundary but inside martensite layer as indicated by arrows in (b) and (d). Histograms of strain in ferrite and martensite layer calculated from Fig. 5(b) and (d) are almost the same between them as shown in Fig. 6. The strain distributions in Fig. 5(a) and (b) were almost the same, therefore, high strain regions at an early stage of deformation are preferentially deformed even at a late stage of deformation. Fig. 7 shows scanning electron microscopy images in before (a) and after 14 % tensile deformation (b) within black dash square region in Fig. 5(b) where strain concentrates. There were no defects or characteristic points at high strained martensite layer before deformation (a), and necking had occurred at the martensite layer after 14 % tensile deformation (b). Fig. 8 shows scanning electron microscopy images on the fracture surface (a), (b) and transverse direction surface (c) after tensile test. Two kinds of fracture surface were observed: One fracture surface consists of fine dimples which correspond to martensite layer due to the width of the region, another fracture surface consists of coarse and shallow

dimples or cleavage-like facets at ferrite layer. Scanning electron microscopy image on transverse direction surface (c) indicated that voids formed in martensite layer or at ferrite/martensite interface as shown by white arrows.

Deformation and fracture model in the multi-layered steel was schematically described in Fig. 9. Ferrite and martensite layers are deformed simultaneously and high strain is continuously distributed along 45 degrees from tensile direction regardless of the layers. Necking occurs at high strained martensite layer and then voids are formed from the region. Finally, coalescence of voids with forming secondary voids in ferrite layer lead to fracture in a multilayered steel. Therefore, it can be concluded that deformability and ductility of hard layer play an important role in the deformation and fracture behavior in a multilayered steel.

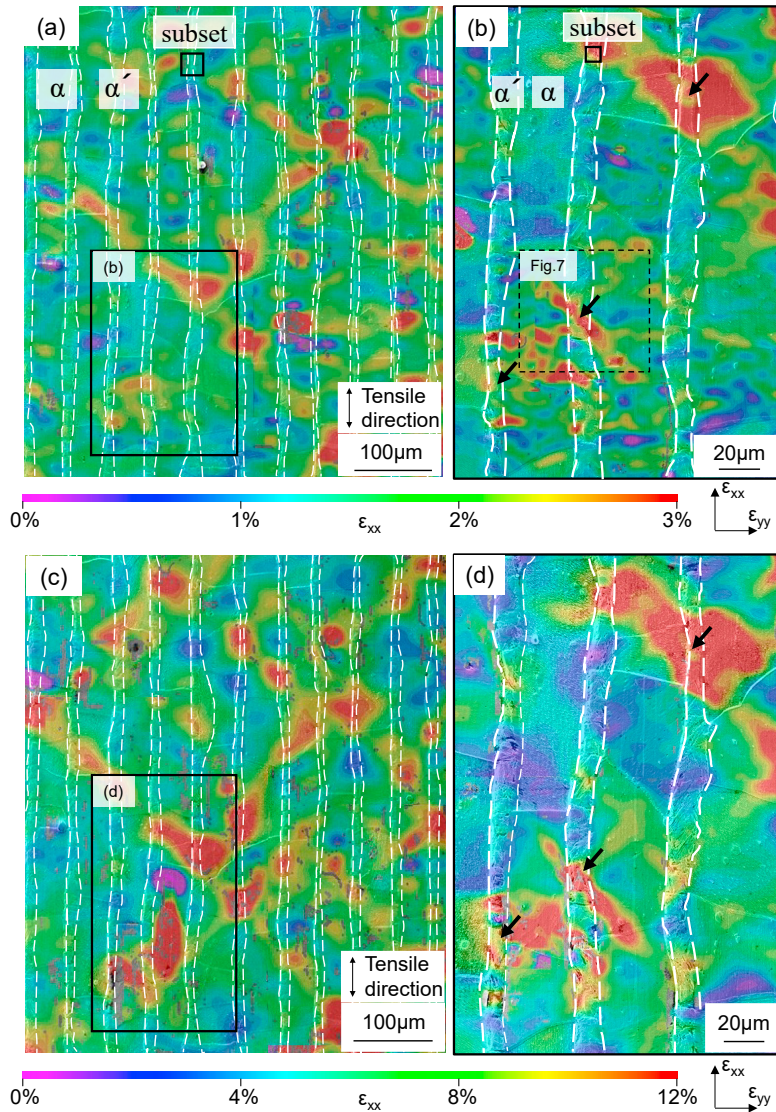


Fig. 5.  $\epsilon_{xx}$  strain distribution in low and high magnification scanning electron microscopy images after (a),(b) 1.6 % and (c), (d) 7.2 % tensile strain in multilayered steel.



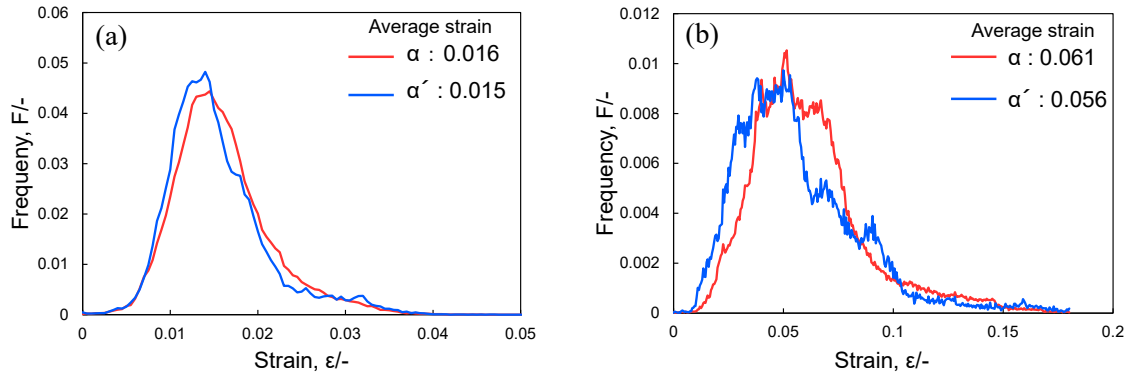


Fig. 6. Histograms of strain in each layer in (a) 1.6 % and (b) 7.4% tensile deformation calculated from Fig. 5(b) and (d).

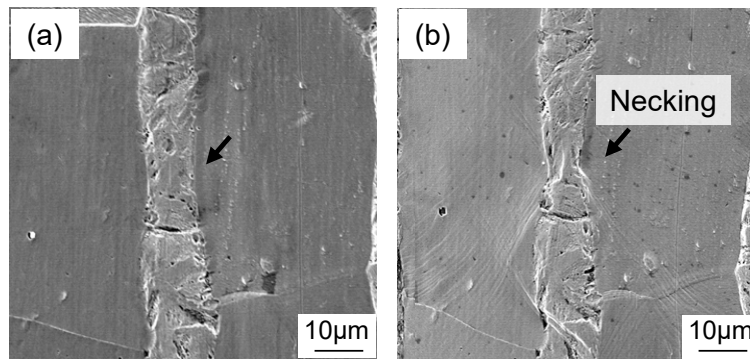


Fig. 7. Scanning electron microscopy images (a) before deformation and (b) after 14 % tensile deformation.

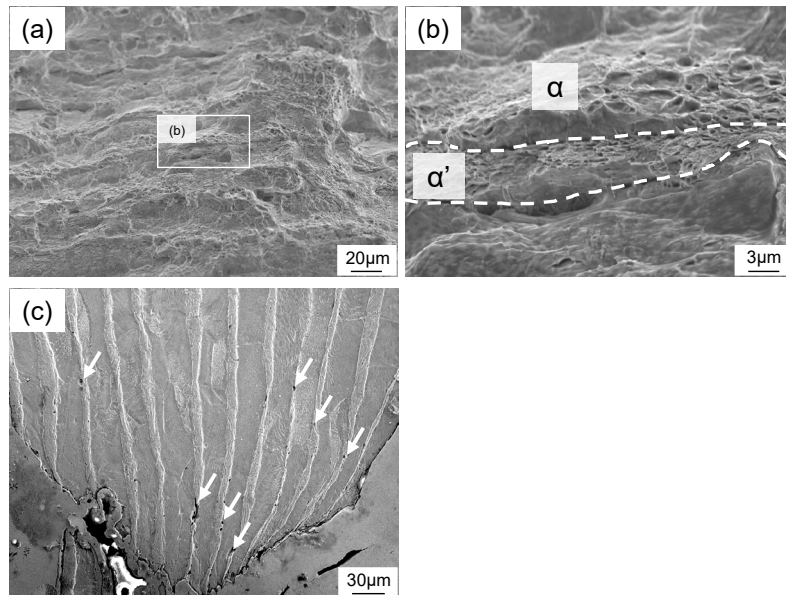


Fig. 8. Scanning electron microscopy images of (a), (b) fracture surfaces and (c) transverse direction surface.

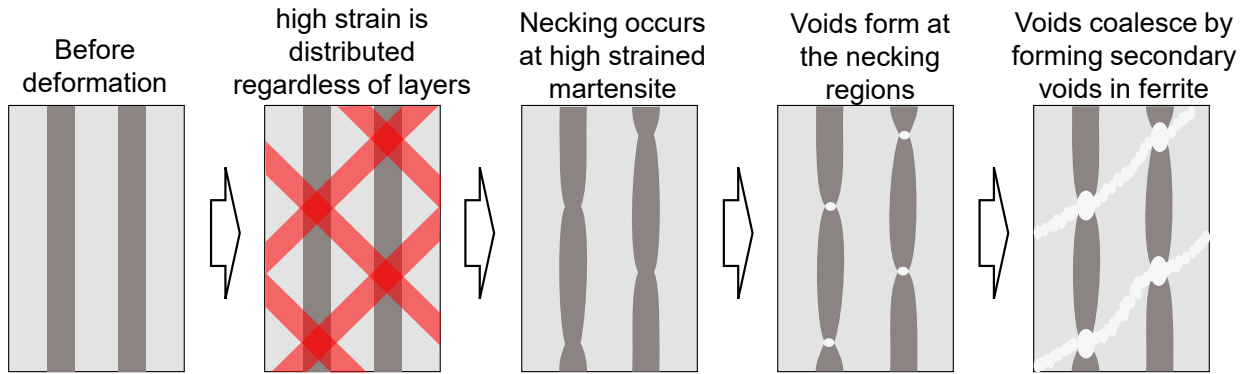


Fig. 9. Schematic illustration of deformation and fracture model in a multi-layered steel.

#### 4. Summary

Ferrite and martensite layers aligned along the rolling direction and there were no peel off or voids at ferrite/martensite interface. Hardness of martensite layer was over twice as much as that of ferrite layer. Inhomogeneous strain distribution was installed by tensile deformation: high strain region was over twice as much as average strain and low strain region was almost 0. Strain was continuously distributed along 45 degrees from the tensile direction regardless of the layers and average strain in ferrite and martensite layer was almost same. Therefore, ferrite and martensite were simultaneously deformed despite of significant difference of hardness between these layers. Necking occurs at high strained martensite layers and then voids formed from the region. Coalescence of voids with forming secondary voids in ferrite layer lead to fracture. Martensite layer was strain concentration site and void nucleation site, therefore, it can be concluded that deformability and ductility of hard layer play an important role in the deformation and fracture in a multilayered steel.

#### 5. Reference

- [1] T. Koseki, J. Inoue, S. Nambu, Development of multilayer steels for improved combinations of high strength and high ductility, *Materials Transactions*, 55 (2014) 227–237.
- [2] J.Y. Koo, M.J. Yong, G. Thomas, On the law of mixtures in dual-phase steels, *Metallurgical and Materials Transactions*, 11 (1980) 852–854.
- [3] M. Ojima, J. Inoue, S. Nambu, P. Xu, K. Akita, H. Suzuki, T. Koseki, Stress partitioning behavior of multilayered steels during tensile deformation measured by in situ neutron diffraction, *Scripta Materialia*, 66 (2012) 139–142.
- [4] N. Jia, Z.H. Cong, X. Sun, S. Cheng, Z.H. Nie, Y. Ren, P.K. Liaw, Y.D. Wang, An in situ high-energy X-ray diffraction study of micromechanical behavior of multiple phases in advanced high-strength steels, *Acta Materialia*, 57 (2007) 3965–3977.
- [5] T.C. Chu, W.F. Ranson, M.A. Sutton, W.H. Peters, Applications of Digital-Image-Correlation techniques to experimental mechanics, *Experimental Mechanics*, 25 (1985) 232–244.
- [6] M.A. Sutton, M.Q. Cheng, W.H. Peters, Y.J. Chao, S.R. McNeill, Application of optimized digital correlation method to planar deformation analysis, *Image and Vision Computing*, 4 (1986) 143–150.
- [7] A. Kotousov, Z. He, A. Fanciulli, Application of digital image correlation technique for investigation of the displacement and strain fields within a sharp notch, *Theoretical and Applied Fracture Mechanics*, 79 (2015) 51–57.
- [8] N. Nakada, M. Nishiyama, N. koga, T. Tsuchiyama, S. Takaki, Hierarchical strain distribution analysis formed in dual phase steel using a combination of metallographic image and digital image correlation method, *Tetsu-to-Hagane*, 100 (2014) 58–65.
- [9] J. Kadkhodapour, A. Butz, S.Z. Rad, Mechanisms of void formation during tensile testing in a commercial, dual-phase steel, *Acta Materialia*, 59 (2011) 2575–2588.
- [10] S. Morito, H. Tanaka, R. Konishi, T. Furuhashi, T. Maki, The morphology and crystallography of lath martensite in Fe-C alloys, *Acta Materialia*, 51 (2003) 1789–1799.
- [11] K. Sasaki, M. Kamaya, T. Miura, K. Fukuya, Correlation between microstructural scale plastic strain and misorientation, *Journal of the Japan Institute of Metals and Materials*, 74 (2010) 467–474.
- [12] R. Tabata, H. Tsuruzono, S. Sadamatsu, Y. Adachi, Digital image correlation analysis of plastic deformation behavior of ferrite in Fe-Mn-Si alloy, *NETSUSHORI*, 55 (2015) 368–377.